BIBLIOGRAPHIC INFORMATION SYSTEM

JOURNAL FULL TITLE: Journal of Biomedical Research & Environmental Sciences
ABBREVIATION (NLM): J Biomed Res Environ Sci **ISSN:** 2766-2276 **WEBSITE:** https://www.jelsciences.com

SCOPE & COVERAGE

- **Sections Covered:** 34 specialized sections spanning 143 topics across Medicine, Biology, Environmental Sciences, and General Science
- Ensures broad interdisciplinary visibility for high-impact research.

PUBLICATION FEATURES

- **Review Process:** Double-blind peer review ensuring transparency and quality
- **Time to Publication:** Rapid 21-day review-to-publication cycle
- **Frequency:** Published monthly
- **Plagiarism Screening:** All submissions checked with iThenticate

INDEXING & RECOGNITION

- **Indexed in:** Google Scholar, IndexCopernicus (**ICV 2022: 88.03**)
- **DOI:** Registered with CrossRef (**10.37871**) for long-term discoverability
- **Visibility:** Articles accessible worldwide across universities, research institutions, and libraries

OPEN ACCESS POLICY

- Fully Open Access journal under Creative Commons Attribution 4.0 License (CC BY 4.0)
- Free, unrestricted access to all articles globally

GLOBAL ENGAGEMENT

- **Research Reach:** Welcomes contributions worldwide
- **Managing Entity:** SciRes Literature LLC, USA
- **Language of Publication:** English

SUBMISSION DETAILS

- Manuscripts in Word (.doc/.docx) format accepted

SUBMISSION OPTIONS

- **Online:** https://www.jelsciences.com/submit-your-paper.php
- **Email:** support@jelsciences.com, support@jbresonline.com

HOME ABOUT ARCHIVE SUBMIT MANUSCRIPT APC

Vision: The Journal of Biomedical Research & Environmental Sciences (JBRES) is dedicated to advancing science and technology by providing a global platform for innovation, knowledge exchange, and collaboration. Our vision is to empower researchers and scientists worldwide, offering equal opportunities to share ideas, expand careers, and contribute to discoveries that shape a healthier, sustainable future for humanity.

JOURNAL OF BIOMEDICAL RESEARCH & ENVIRONMENTAL SCIENCES
ISSN: 2766-2276
SUBJECT AREA(S): AGRICULTURAL SCIENCES | MICROBIOLOGY
DOI: 10.37871

RESEARCH ARTICLE

Effect of Plant Growth-Promoting Microorganisms against *Fusarium oxysporum* on *Cannabis Sativa*

Sourav Maharaj[1]* and Mbili NC[2]

[1]School of Agricultural, Earth and Environmental Sciences, University of KwaZulu-Natal, Pietermaritzburg, South Africa

[2]Discipline of Plant Pathology, School of Agriculture and Science, University of KwaZulu-Natal, South Africa

Abstract

Fusarium oxysporum is a destructive soilborne pathogen that causes vascular wilt and root rot in *Cannabis sativa*, limiting plant health and productivity under greenhouse production. This study evaluated the antagonistic and growth-promoting effects of plant growth-promoting microorganisms, namely *Trichoderma asperellum*, *Bacillus velezensis*, *Bacillus amyloliquefaciens*, and *Microbacterium proteolyticum*, against a pathogenic *F. oxysporum* isolate *in vitro* and *in vivo*. Dual-culture assays on Potato Dextrose Agar were used to determine inhibitory activity, while scanning electron microscopy was employed to examine pathogen–antagonist interactions. In greenhouse trials, the cannabis cultivar 'Bergville' was pretreated with each microorganism and challenged with *F. oxysporum* to assess disease incidence, disease severity, AUDPC, infection rates, and plant growth responses over 40 days.

All microbial treatments significantly suppressed *F. oxysporum* growth *in vitro* ($p < 0.001$). *B. velezensis*, *B. amyloliquefaciens*, and *M. proteolyticum* showed the strongest inhibition, whereas *T. asperellum* exhibited slower but clear antagonistic activity characterized by hyphal coiling and mycoparasitism. *in vivo*, all inoculated plants developed disease, but *B. amyloliquefaciens* provided the greatest reduction in disease progression, with the lowest AUDPC. *T. asperellum* and *B. velezensis* also reduced disease advancement, while *M. proteolyticum* promoted the greatest plant height despite limited biocontrol efficacy. Bacillus treatments improved leaf number and vegetative vigor, although total root and shoot biomass did not differ significantly among treatments.

These findings indicate that *B. amyloliquefaciens*, *B. velezensis*, and *T. asperellum* are promising biological control agents for sustainable management of *F. oxysporum* in cannabis production.

***Corresponding author(s)**

Sourav Maharaj, School of Agricultural, Earth and Environmental Sciences, University of KwaZulu-Natal, Pietermaritzburg, South Africa
Email: 222002370@stu.ukzn.ac.za

DOI: 10.37871/jbres2311

Submitted: 19 June 2026

Accepted: 29 June 2026

Published: 02 July 2026

Keywords

- Fusarium oxysporum
- *Biocontrol; C*
- Sativa

VOLUME: 7 ISSUE: 7 - JULY, 2026

How to cite this article: Maharaj S, Mbili NC. Effect of Plant Growth-Promoting Microorganisms against Fusarium oxysporum on Cannabis Sativa. J Biomed Res Environ Sci. 2026 June 30; 7(7): 19. Doi: 10.37872/jbres2311

List of Abbreviations

FO: Fusarium oxysporum; TA: Trichoderma asperellum; BA: Bacillus amyloliquefaciens; BV: Bacillus velezensis; MP: Microbacterium proteolyticum; AUDPC: Area under the Disease Progress Curve; BCAs: Bacterial biocontrol agents; CFU: Colony-forming units; CRD: Completely randomized design; DMRT: Duncan's Multiple Range Test; EHT: Accelerating voltage; H_2O: Water; PDA: Potato Dextrose Agar; SE: Standard error; SEM: Scanning Electron Microscopy; WD: Working distance.

Introduction

Fusarium oxysporum is an important soilborne fungal pathogen responsible for vascular wilt and persistent yield losses in a wide range of hosts, including *C. sativa*. In cannabis production, *F. oxysporum* has been associated with root browning, crown infection, yellowing, stunting, and plant death, and it has been recovered from diseased crowns, stems, pith tissues, roots, and even propagation systems, showing how readily it can spread through commercial facilities [1,2]. As greenhouse and controlled-environment cannabis production has expanded, disease pressure has increased alongside it, with *Fusarium* and *Pythium* among the principal root pathogens affecting this crop [1,3].

Management of Fusarium wilt in cannabis remains constrained. Recent reviews note that biopesticides are available for use on *C. sativa*, but few efficacy trials have been performed, and producers still have limited management options in the absence of registered chemical fungicides [3,4]. This has made biological control an increasingly important component of integrated disease management. *Trichoderma* spp. and bacterial biocontrol agents, particularly *Bacillus* spp., are especially promising because they can suppress fungal pathogens through direct antimicrobial activity, competition for nutrients and space, and induction of host systemic resistance [5]. In cannabis systems, *Trichoderma*- and *Bacillus*-based products have reduced disease severity under greenhouse conditions, and beneficial bacteria have also shown activity against Fusarium through dual-culture inhibition and in planta suppression [4,6,7].

Cannabis-specific studies support this direction. In a greenhouse trial, several biological-control products reduced mean disease severity in Fusarium-inoculated cannabis cuttings, with the most effective treatments including *Trichoderma*- and *Bacillus*-based products [4]. A separate study reported that a plant growth-promoting bacterial consortium counteracted Fusarium infection both pre-emergence and post-emergence [8]. Another cannabis study found significant inhibition of *Fusarium oxysporum* mycelial growth by several *Bacillus* strains, further supporting the potential of rhizobacterial antagonists for sustainable disease management [9]. However, the evidence remains fragmented across microbial taxa, formulations, and production systems, and direct comparisons among candidate agents are still scarce [3,10].

Against this background, the present study evaluated *Trichoderma asperellum*, *Bacillus velezensis*, *Bacillus amyloliquefaciens*, and *Microbacterium proteolyticum* against *F. oxysporum* in the cannabis cultivar 'Bergville' under greenhouse conditions. The antagonistic activity of these agents was assessed using dual-culture assays on Potato Dextrose Agar, with Bell's rating scale used to quantify antagonism and scanning electron microscopy employed to examine the physical interactions between the pathogen and the biocontrol agents at the microscopic level [6] By comparing disease progression and growth responses across these antagonists, the study aimed to identify biological control agents with potential for suppressing Fusarium wilt while preserving plant vigour and biomass under pathogen challenge.

This work is novel in that it directly compares multiple microbial antagonists under the same experimental conditions in cannabis, while also combining dual-culture assays, Bell's rating scale, and scanning electron microscopy to characterize both antagonistic performance and pathogen–antagonist interactions.

The practical significance of the study lies in its potential to identify biologically based options for Fusarium wilt management in cannabis, where effective disease-control tools remain limited.

Specifically, the study aimed to determine which of the tested biocontrol agents most effectively suppresses *F. oxysporum* while maintaining plant vigour and biomass under pathogen challenge.

The *Trichoderma asperellum* isolate used in this study was obtained from EcoT®, whereas the bacterial species were isolated from soil and sent to Inqaba Biotechnical Industries (Pty) Ltdfor sequencing and identification to a species level.

Methods and Materials

Bell's test for Trichoderma asperellum vs F. oxysorum

To assess the antagonistic interaction between T. asperellum and the pathogenic fungus F. oxysporum, a dual culture assay was performed using Potato Dextrose Agar (PDA) in Petri plates (Figure 1). A 5 mm mycelial plug of F. oxysporum was inoculated on one side of the PDA plate, and a plug of T. asperellum was placed on the opposite side, equidistant from the center. The plates were incubated at 25°C (room temperature) for 3-7 days, after which the interaction between the two fungi was evaluated using Bell's rating scale. This scale ranges from 1 to 5, where a rating of 1 indicates that Trichoderma completely overgrew the pathogen, covering the entire plate, and a rating of 5 indicates complete overgrowth of Trichoderma by the pathogen with no inhibition observed. Intermediate ratings reflect varying levels of growth and inhibition between the two organisms. Lower scores (1–2) denote strong antagonism by Trichoderma, whereas higher scores (4–5) indicate weak or no antagonistic effect.

In vitro Antagonism Assay Between F.

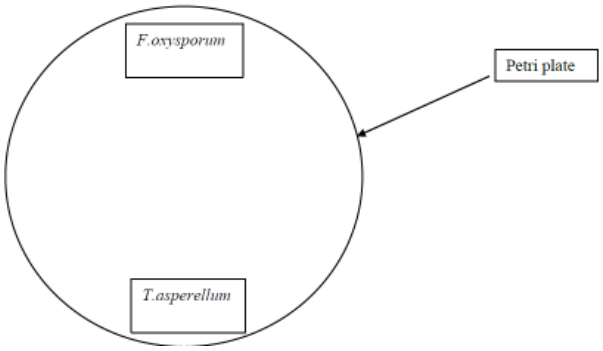

Figure 1 Dual culture assay showing antagonistic interaction between F. oxysporum and T. asperellum on Potato Dextrose Agar (PDA). A mycelial plug of *F. oxysporum* was placed on one side of the Petri plate, while a plug of T. asperellum was inoculated on the opposite side. The interaction zone between the two fungi was observed after incubation and rated using Bell's scale to assess the level of antagonism.

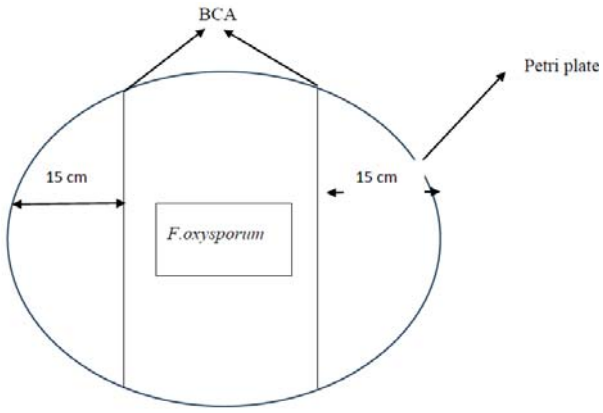

Figure 2 Schematic representation of the in vitro antagonism assay between *F. oxysporum* and bacterial biocontrol agents (BCAs). A 5 mm plug of *F. oxysporum* was placed at the center of a Petri plate containing a suitable growth medium, while bacterial isolates were streaked equidistantly around the periphery. The setup was incubated at 25–30°C for 3–7 days to observe inhibitory interactions such as growth suppression, zones of inhibition, or morphological changes in the fungal colony.

oxysporum and Bacterial Isolates

To evaluate the antagonistic potential of bacterial isolates against *F. oxysporum*, a dual culture bioassay was performed on Petri dishes containing a suitable growth medium, PDA. Each plate was first labelled and marked on the bottom to indicate the central point for fungal inoculation and the positions around the edge for bacterial streaks. A 5 mm agar plug of actively growing *F. oxysporum* culture was placed at the center of the plate using sterile forceps or a scalpel. Pure bacterial cultures were then streaked using a sterile inoculating loop in straight lines, starting 15cm away from the edge of the plate (Figure 2). Bacterial species used include *Bacillus velezensis*, *Bacillus amyloliquefaciens* and *Microbacterim proteolyticum.* Plates were incubated at 25˚C for 3-7 days. Post incubation, the interaction zones were carefully observed for evidence of antagonism, such as clear zones of inhibition, overgrowth, pigment production, or changes in fungal morphology near the bacterial streaks. Observations included the distance between growth fronts and any visible signs of hyphal degradation, which served as indicators of the biocontrol efficacy of the bacterial isolates.

Control Culture Preparation of F. oxysporum

To establish a control for fungal growth, **F. oxysporum** was cultured on PDA in sterile Petri dishes. Each plate was labelled on the bottom with "*F. oxysporum* Control," along with the date and initials. Using cork borer, a 5 mm agar plug was excised from the actively growing edge of a **F. oxysporum** culture. The plug was then transferred to the center of a fresh PDA plate using sterile forceps, ensuring the mycelium side was in contact with the medium. The plates were sealed with parafilm to prevent contamination and desiccation, while allowing minimal gas exchange. Plates were incubated at 25˚C for 3-7 days. Radial growth from the center was measured at intervals in millimetres, and colony characteristics such as colour, texture, sporulation, and pigment production were recorded for comparative analysis with treated plates.

Scanning Electron Microscopy (SEM)

Scanning Electron Microscopy (SEM) was conducted to observe and compare the surface morphology of the samples. Samples were first fixed in 3% buffered glutaraldehyde for 1–3 hours to preserve cellular and structural integrity. Following fixation, samples were dehydrated gradually through a graded ethanol series consisting of 10%, 30%, 50%, 70% and 90% ethanol for 10 minutes each, followed by three final washes in 100% ethanol to ensure complete removal of water. The fully dehydrated samples were then subjected to critical point drying using a Quorum K850 Critical Point Dryer, where ethanol was progressively replaced with liquid CO_2 and subsequently brought to its critical point (~35˚C and ~1200–1300 psi), allowing the transition from liquid to gas without surface tension forces that could otherwise collapse or distort fine surface structures. Once dried, the samples were mounted on aluminium SEM stubs using carbon adhesive tabs, ensuring proper orientation and secure placement. A thin conductive layer of gold was then applied using a Quorum Q150RES Sputter Coater to enhance surface conductivity and minimize charging during electron beam exposure. The prepared samples were examined using a Zeiss EVO LS15 scanning electron microscope operated under high-vacuum conditions at an accelerating voltage appropriate for biological specimens. Micrographs were captured at multiple magnifications to visualise overall surface architecture as well as fine microstructural features relevant to the study. This imaging approach enabled detailed comparison of fungal colony morphology on PDA plates, allowing assessment of differences in hyphal structure, surface texture, and growth characteristics between treatments.

Plant material and xperimental setup

The cannabis cultivar 'Bergville' was used for all *in vivo* trials. Healthy, uniform seedlings were grown under controlled greenhouse conditions to ensure consistent growth prior to treatments.

Preparation of Biological Control Agents (BCAs)

Pure cultures of Trichoderma asperellum, Bacillus velezensis, Bacillus amyloliquefaciens, and Microbacterium proteolyticum were obtained from microbial culture collections. Each BCA was cultured in PDA, and spore or cell suspensions were prepared and standardized to a concentration of 1×10^8 colony-forming units (CFU)/mL for bacterial agents and 1×10^8 spores/mL for fungal agents.

Pathogen Preparation

F. oxysporum was cultured on PDA plates and incubated at 25°C for 7 days. Spore suspensions were harvested and adjusted to 1×10^5 conidia/mL for inoculation.

Inoculation Procedure

Prior to inoculation, 'Bergville' seedlings were stressed by covering with plastic bags for 24 hours to create a high-humidity environment that weakens plant defenses. Following this stress period, each plant was treated with a soil drench of 20 mL of the respective biological control agent suspension at 1×10^8 CFU/mL or spores/mL around the root zone. After 48 hours, plants were inoculated by soil drenching with 20 mL of F. oxysporum spore suspension adjusted to 1×10^5 conidia/mL. Control groups included stressed plants treated only with pathogen inoculum and stressed plants receiving sterile distilled water.

Experimental Design

The experiment was conducted in a completely randomized design (CRD) comprising six treatment groups with three replications per treatment and three pots per replication, totalling 54 pots. The treatment groups were as follows:

- **(F. oxysporum) + (Trichoderma asperellum)**
- **(F. oxysporum) + (Bacillus velezensis)**
- **(F. oxysporum) + (Bacillus amyloliquefaciens)**
- **(F. oxysporum) + (Microbacterium proteolyticum)**
- **(F. oxysporum only** (positive control))
- **(Sterile water only** (negative control))

Data Collection

Plants were monitored for disease incidence and severity, as well as growth parameters such as plant height, leaf number, vascular wilting over a period of forty days. Other parameters such as dry root mass. Disease severity was scored using a standard rating scale. Plant and root wet and dry mass was recorded. Plant material was dried for 48 hours at 65°C in an industrial plant oven. Disease severity in the greenhouse trials was assessed using a standardized rating scale (1-5), allowing comparison of symptom development across treatments under identical controlled conditions.

Statistical analysis

Data were subjected to ANOVA and means were separated using Duncan's Multiple Range Test.

Results

The ANOVA results (Table 1) show that treatments had a highly significant effect ($p < 0.001$) on the mycelial growth of F. oxysporum at day 3, with a very large variance ratio (v.r. = 494.51). Replicates had no significant effect, and

most of the variation in growth was explained by the treatment differences rather than random error.

The ANOVA results (Table 2) indicate that treatments had a highly significant effect ($p < 0.001$) on the mycelial growth of F. oxysporum at day 5, with an extremely high variance ratio (v.r. = 951.48). Replicates showed no significant effect, and almost all variation in growth was attributed to treatment differences rather than experimental error.

The ANOVA results (Table 3) show that treatments had a highly significant effect ($p < 0.001$) on the mycelial growth of F. oxysporum at day 7, with a very high variance ratio (v.r. = 879.71). Replicates had no significant effect, and the majority of variation in growth was due to treatment differences rather than random error.

The bar graph (Figure 3) shows the mean mycelial growth of F. oxysporum under five treatments (BA, BV, FO, MP, TA) at 3-, 5-, and 7-days post-inoculation. Growth was highest in the FO treatment (~80 mm) across all days, while BA, BV, and MP exhibited much lower growth (~30–40 mm). TA showed moderate growth (~40 mm on day 3, increasing to ~60 mm by day 7). Error bars indicate standard error, with FO displaying the greatest and most consistent growth over time, and TA showing noticeable increases between days 3 and 7 (Table 4).

The analysis of variance (Table 5) shows that there were no significant differences ($p > 0.05$) among treatments in root wet mass of *C. sativa*. This indicates that the application of the different biological control agents and combinations did not significantly affect the water-holding capacity or fresh weight of the roots. Although numerical variations were observed between treatments, these were not statistically meaningful, suggesting that the treatments maintained a relatively similar influence on belowground biomass accumulation under the experimental conditions.

Table 1: Analysis of Variance (ANOVA) Table for Treatment Effects on Mycelial Growth of F. oxysporum day 3.

Source of variation	d.f.	s.s.	m.s.	v.r.	F pr.
REPLICATES stratum	2	3.80	1.90	0.13	
REPLICATES.*Units* stratum TREATMENTS	4	29919.18	7479.79	494.51	<.001
Residual	83	1255.42	15.13		
Total	89	31178.40			

Table 2: Analysis of Variance (ANOVA) Table for Treatment Effects on Mycelial Growth of F. oxysporum day 5.

Source of variation	d.f.	s.s.	m.s.	v.r..	F pr.
REPLICATES stratum	2	5.356	2.678	0.37	
REPLICATES.*Units* stratum TREATMENTS	4	27351.156	6837.789	951.48	<.001
Residual	83	596.478	7.186		
Total	89	27952.989			

Table 3: Analysis of Variance (ANOVA) Table for Treatment Effects on Mycelial Growth of F. oxysporum day 7.

Source of variation	d.f.	s.s.	m.s.	v.r.	F pr.
REPLICATES stratum	2	4.356	2.178	0.29	
REPLICATES.*Units* stratum TREATMENTS	4	26680.156	6670.039	879.71	<.001
Residual	83	629.311	7.582		
Total	89	27313.822			

Table 4: Average disease incidence (%) recorded for each treatment over the experimental period from 10 September to 13 October. Treatments include T. asperellum (TA), B. velezensis (BV), B. amyloliquefaciens (BA), M. proteolyticum (MP), F. oxysporum (FO), and the water control (H_2O).

Treatment	10-Sep	13-Sep	16-Sep	19-Sep	22-Sep	25-Sep	28-Sep	1-Oct	4-Oct	7-Oct	10-Oct	13-Oct
TA	100	100	100	100	100	100	100	100	100	100	100	100
BV	100	100	100	100	100	100	100	100	100	100	100	100
BA	100	100	100	100	100	100	100	100	100	100	100	100
MP	100	100	100	100	100	100	100	100	100	100	100	100
FO	100	100	100	100	100	100	100	100	100	100	100	100
H_2O	0	0	0	0	0	0	0	0	0	0	0	0

Table 5: Analysis of variance (ANOVA) for root wet mass of C. sativa under different treatments, as computed using Genstat 23rd Edition.

Source of variation	d.f.	s.s.	m.s.	v.r.	F pr.
Replicate stratum	2	31.46	15.73	0.36	
Replicate.*Units* stratum					
Treatment	5	134.00	26.80	0.62	0.688
Residual	46	2002.22	43.53		
Total	53	2167.69			

Table 6: Analysis of variance (ANOVA) for plant mass of C. sativa under different treatments, as computed using Genstat 23rd Edition.

Source of variation	d.f.	s.s.	m.s.	v.r.	F pr.
Replicate stratum	2	31.96	15.98	1.03	
Replicate.*Units* stratum					
Treatment	5	54.79	10.96	0.71	0.621
Residual	46	712.34	15.49		
Total	53	799.09			

Table 7: Analysis of variance (ANOVA) for root dry mass of C. sativa under different treatments, as computed using Genstat 23rd Edition.

Source of variation	d.f.	s.s.	m.s.	v.r.	F pr.
Replicate stratum	2	0.341	0.171	0.12	
Replicate.*Units* stratum					
Treatment	5	5.813	1.163	0.81	0.547
Residual	46	65.813	1.431		
Total	53	71.967			

Table 8: Analysis of variance (ANOVA) for plant dry mass of C. sativa under different treatments, as computed using Genstat 23rd Edition.

Source of variation	d.f.	s.s.	m.s.	v.r.	F pr.
Replicate stratum	2	6.459	3.230	1.80	
Replicate.*Units* stratum					
Treatment	5	4.824	0.965	0.54	0.746
Residual	46	82.484	1.793		
Total	53	93.767			

Figure 17 illustrates the mean root wet mass of *C. sativa* plants subjected to different treatments. The error bars represent the standard error of the mean (±SE), and the absence of different letters above the bars indicates no significant differences according to Duncan's Multiple

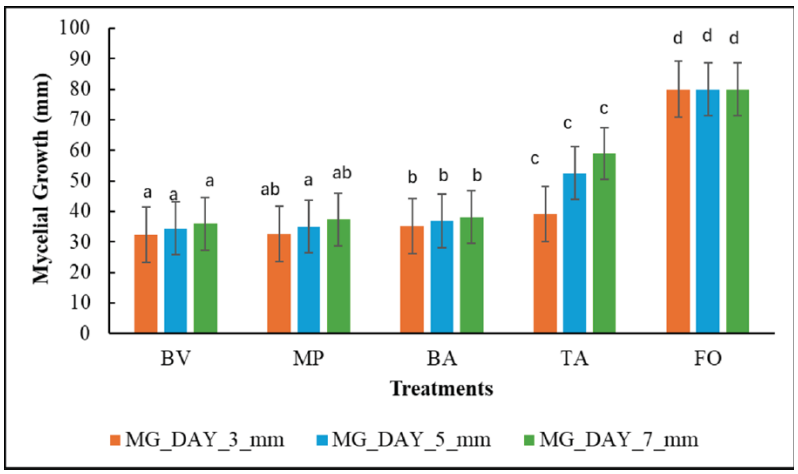

Figure 3 Mean mycelial growth (mm) of F. oxysporum on different treatments (BA, BV, FO, MP, TA) measured at 3-, 5-, and 7-days post-inoculation. Data represent means ± standard error as calculated using GenStat® 23rd Edition.

Range Test (DMRT). Overall, the figure shows that root wet mass remained relatively consistent across treatments, suggesting that the various microbial inoculations and control treatments had a comparable effect on root moisture and development. This consistency may imply that all treatments supported similar water uptake and retention capacity in the roots.

The ANOVA results in table 6 indicate that there were no significant differences ($p > 0.05$) in plant wet mass among the six treatments tested. This finding suggests that the treatments had little to no measurable effect on the total fresh biomass accumulation of *C. sativa*. The uniformity in wet mass values implies that plant growth and water content in aerial tissues (stems and leaves) were not significantly influenced by the application of biological control agents compared to the untreated control.

As shown in figure 18, the mean plant wet mass of *C. sativa* exhibited minimal variation among treatments, with no significant differences detected by DMRT ($p > 0.05$). The graph shows that all treatments resulted in comparable levels of fresh plant biomass, reflecting similar growth responses under the same environmental conditions. The consistent pattern of wet mass suggests that while the microbial treatments may have contributed to plant vigor, their effects on overall plant hydration and mass accumulation were not statistically distinct.

According to the ANOVA results in table 7, there were no statistically significant differences ($p > 0.05$) in root dry mass among the treatments. This indicates that the treatments did not significantly alter the accumulation of dry matter in *C. sativa* roots. The close similarity in mean square and sum of squares values

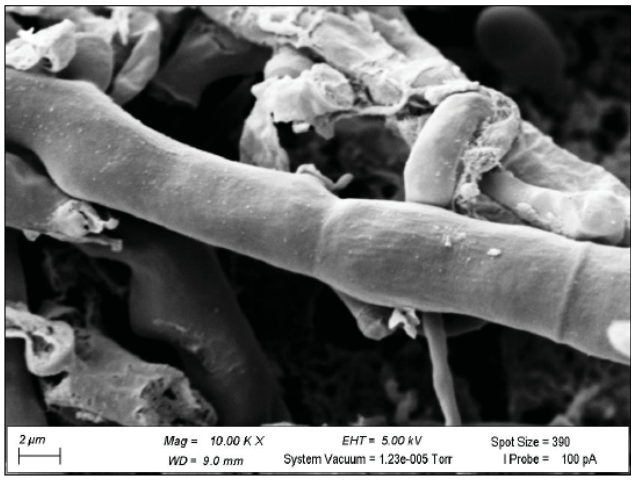

Figure 4 Scanning electron micrograph (SEM) of *F. oxysporum* isolated from C. sativa showing hyphal structures at 10,000× magnification. The image reveals smooth, septate hyphae with visible branching and intertwined mycelial networks, characteristic of the fungal morphology. Imaging was performed at an accelerating voltage of 5.00 kV and a working distance of 9.0 mm.

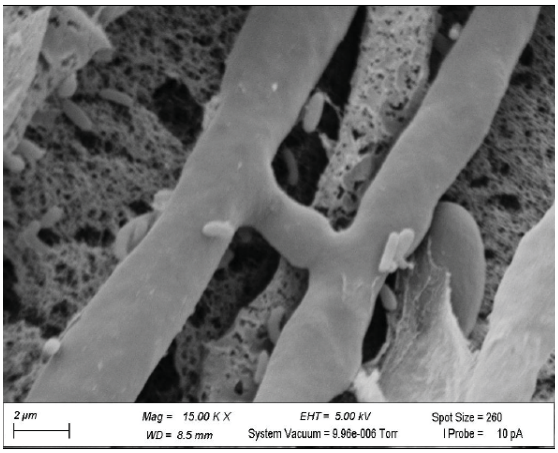

Figure 5 Scanning electron micrograph (SEM) of *F. oxysporum* isolated from C. sativa showing septate hyphae with branching and attached microconidia at 15,000× magnification. The smooth, tubular hyphal structures and ellipsoidal conidia are clearly visible, characteristic of F. oxysporum morphology. Imaging was performed at an accelerating voltage of 5.00 kV and a working distance of 8.5 mm.

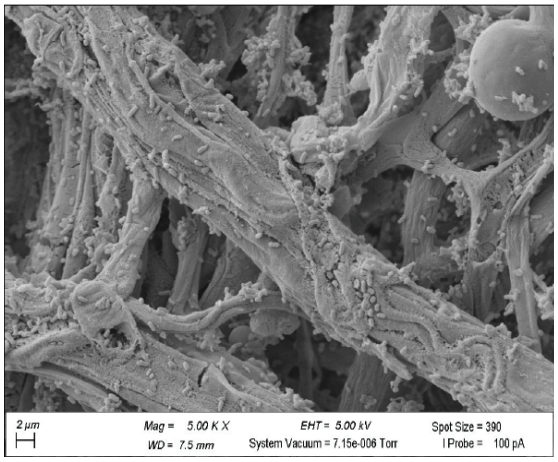

Figure 6 Scanning electron micrograph (SEM) showing the interaction between T. asperellum and *F. oxysporum* at 5,000× magnification. The image reveals extensive hyphal intertwining, coiling, and surface colonization, with numerous conidia of T. asperellum visible on and around the *F. oxysporum* hyphae, indicating antagonistic activity. Imaging was performed at an accelerating voltage of 5.00 kV and a working distance of 7.5 mm.

across treatments suggests a uniform effect, where each treatment supported comparable root biomass production after drying, implying that microbial inoculation had a neutral effect on root structural growth.

Figure 19 presents the mean root dry mass values for *C. sativa* under the different treatments. The results show a similar trend across all treatments, with overlapping error bars and no significant differences according to DMRT. These findings suggest that the treatments did not differentially affect root biomass accumulation after moisture removal. The data imply that despite the potential for plant growth-promoting microorganisms to enhance nutrient uptake and root development, their influence on final dry root mass under the given conditions was not significant.

The ANOVA results in table 8 reveal that there were no significant differences ($p > 0.05$) in total plant dry mass among treatments. This suggests that the various treatments, including biological control agents, did not significantly

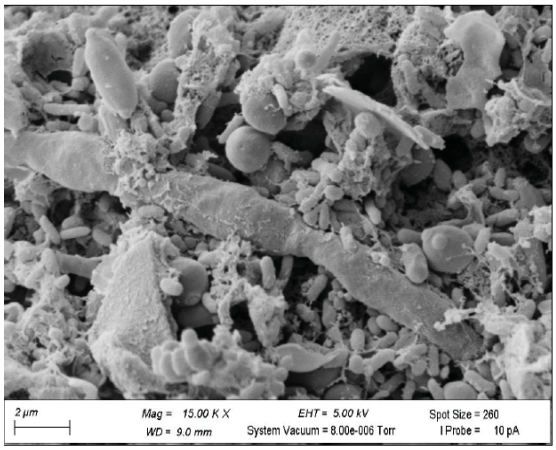

Figure 7 Scanning Electron Micrograph (SEM) of the interaction between B. velezensis and *F. oxysporum* isolated from *C. sativa*. The image, captured at 15.00K X magnification, clearly shows the co-existence of different microbial forms. Rod-shaped bacterial cells (*B. velezensis*) are densely clustered and adhere to the surfaces of larger, elongated fungal hyphae and spherical to ovoid fungal spores/conidia (characteristic structures of *F. oxysporum*). A significant amount of visible extracellular matrix (biofilm) surrounds the organisms, suggesting active colonization and potential antagonistic interaction between the bacteria and the fungus. Imaging was performed at an accelerating voltage (EHT) of 5.00 kV and a working distance (WD) of 9.0mm. The scale bar represents 2µm.

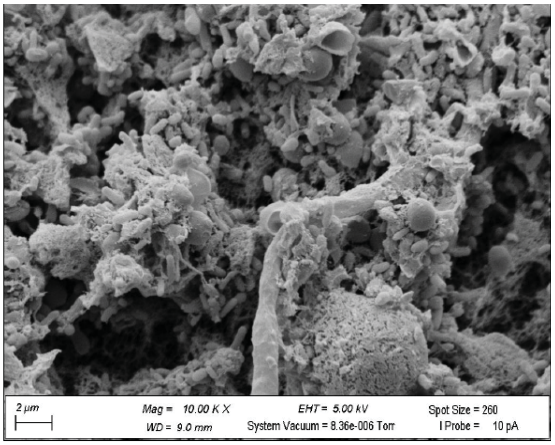

Figure 8 Scanning Electron Micrograph (SEM) of the interaction between B. velezensis and *F. oxysporum* isolated from C. sativa. The image, captured at 10.00K X magnification, illustrates a dense, mixed microbial community. A dominant thick fungal hypha (*F. oxysporum*) is visible, surrounded and heavily coated by numerous rod-shaped bacterial cells (*B. velezensis*). Spherical to ovoid fungal spores/conidia are also present, embedded within an extensive network of extracellular matrix (biofilm) material. This close association suggests active antagonism or biocontrol activity of the bacterium against the pathogenic fungus. Imaging was performed at an accelerating voltage (EHT) of 5.00 kV and a working distance (WD) of 9.0mm. The scale bar represents 2µm.

influence the total dry biomass yield of *C. sativa.* The uniformity across replicates and treatments indicates that the plants maintained consistent growth and dry matter partitioning, regardless of the microbial treatments applied.

The graph (Figure 21) compares the final disease severity across six different treatments. The highest disease severity percentages (over 60%) were observed for treatments MP and FO, with FO showing the maximum severity, suggesting they represent the conditions most conducive to disease or the application of the pathogen. Treatments TA, BV, and BA resulted in moderate disease severity (ranging from approximately 43% to 53%), indicating a partial effect. In contrast, the Water control exhibited negligible disease severity (0%), confirming the baseline disease level in the absence of the applied treatments or inoculum.

Discussion

Figure 9 Macroscopic morphology of a pathogenic *F. oxysporum* isolate recovered from inflorescences (flowers) of a 'Blueberry Cannabis' plant. The culture, grown on PDA, exhibits the typical fast-growing colony with dense, cottony (floccose) aerial mycelium. The colony often develops a light pink or purple pigmentation visible in the mycelium or on the reverse side of the Petri dish, indicative of a *Fusarium* species. This isolate is associated with vascular wilt of C. sativa.

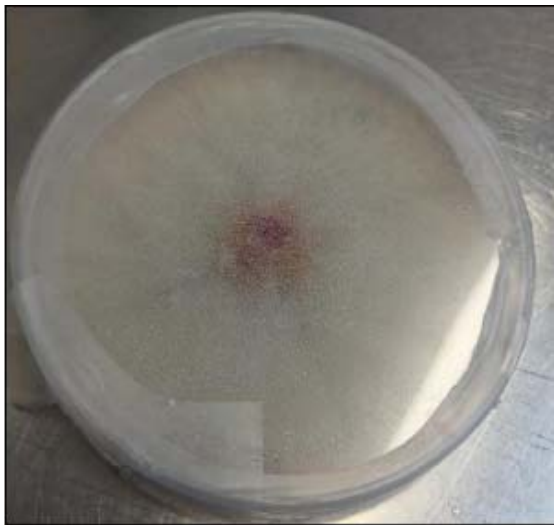

Figure 10 Pure culture of F. *oxysporum* grown on Potato Dextrose Agar (PDA). Note the characteristic fluffy, white to pinkish aerial mycelium on the upper surface and the deep purple pigmentation observed on the reverse of the plate.

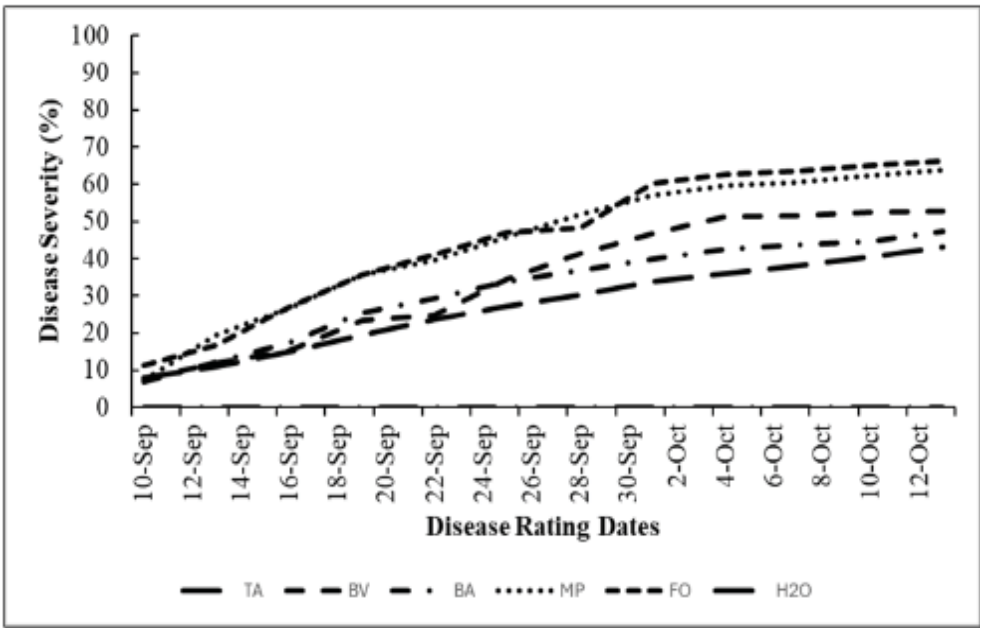

Figure 11 Average Disease Severity over Time for Various Treatments. The graph illustrates the progression of disease severity (as a percentage, %) measured across different "Disease Rating Dates" (from September 10 to October 12). Disease severity increases for all groups over the monitoring period. The treatments are differentiated by line style: TA (thin solid line), BV (long dashed line), BA (dash-dot line), MP (dotted line), FO (medium dashed line), and H2O (thick solid line). The lines show the relative efficacy of each treatment in managing the disease, with the H2O (water) and FO treatments generally resulting in the highest disease severity, while the TA and BV treatments show lower severity.

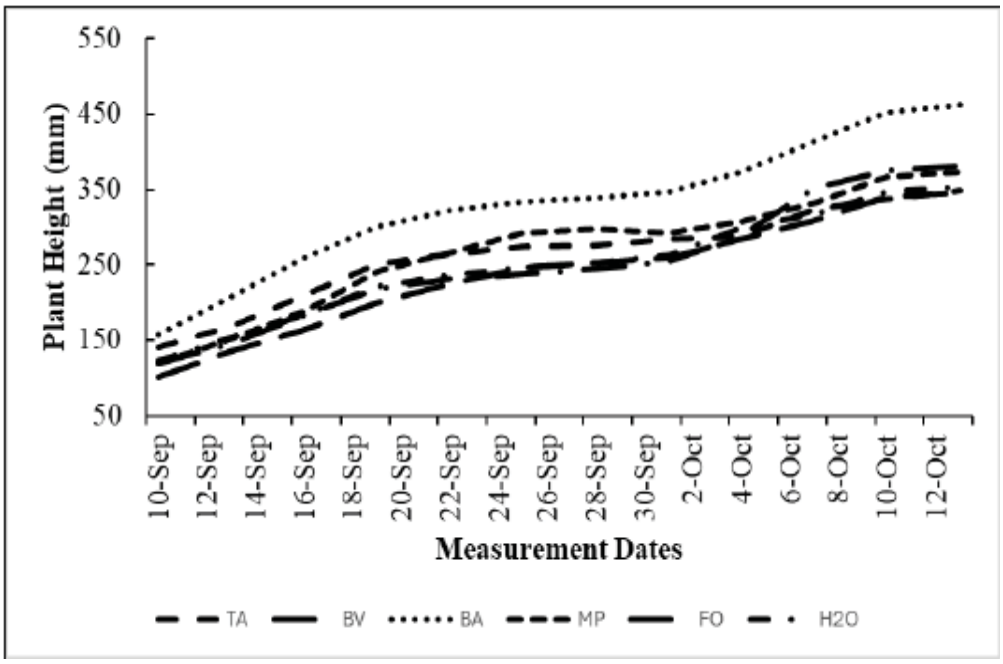

Figure 12 Average Plant Height Over Time for Various Treatments. The graph tracks the mean plant height (measured in millimeters, mm) for different treatments across the "Measurement Dates" (from September 10 to October 12). Plant height consistently increased in all treatment groups throughout the study period. The treatments are represented by line styles: TA (thin solid line), BV (long dashed line), BA (dash-dot line), MP (dotted line), FO (medium dashed line), and H2O (thick solid line). The MP (dotted line) treatment resulted in the greatest overall plant height, suggesting a potential plant growth promotion effect compared to the other treatments, including the control.

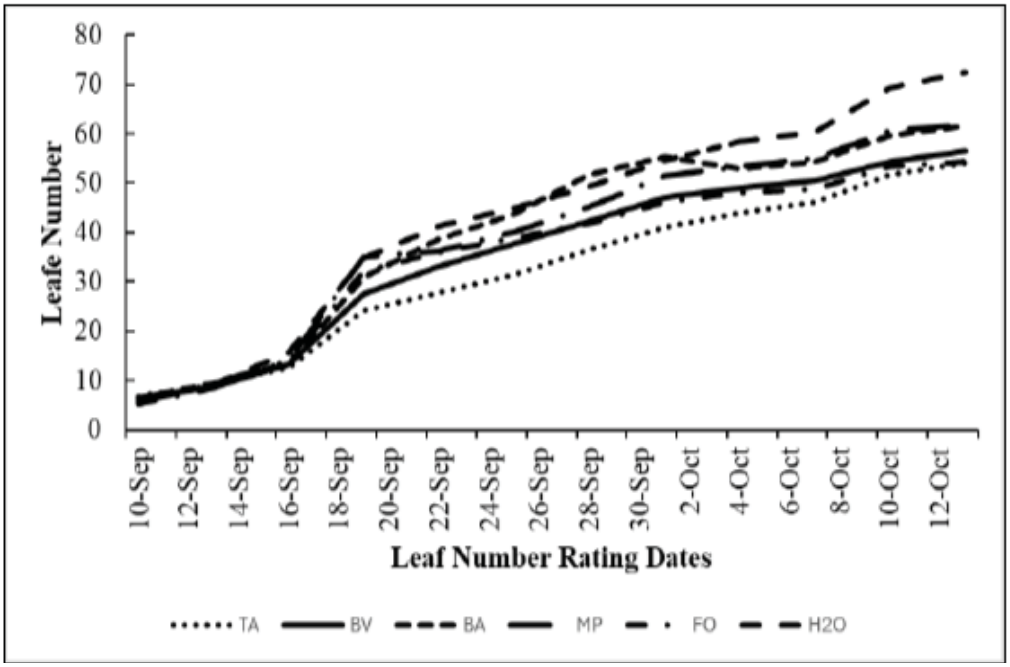

Figure 13 Average Leaf Number Over Time for Various Treatments. The graph presents the mean "Leaf Number" count recorded for different treatments across the "Leaf Number Rating Dates" (from September 10 to October 12). The leaf count increased steadily for all groups throughout the period. The treatments are indicated by line style: TA (dotted line), BV (thick solid line), BA (long dashed line), MP (dash-dot line), FO (medium dashed line), and H2O (thin solid line). The BA and BV treatments resulted in the highest overall leaf counts by the end of the experiment, suggesting they may have a beneficial effect on plant growth, while the TA treatment resulted in the lowest leaf numbers.

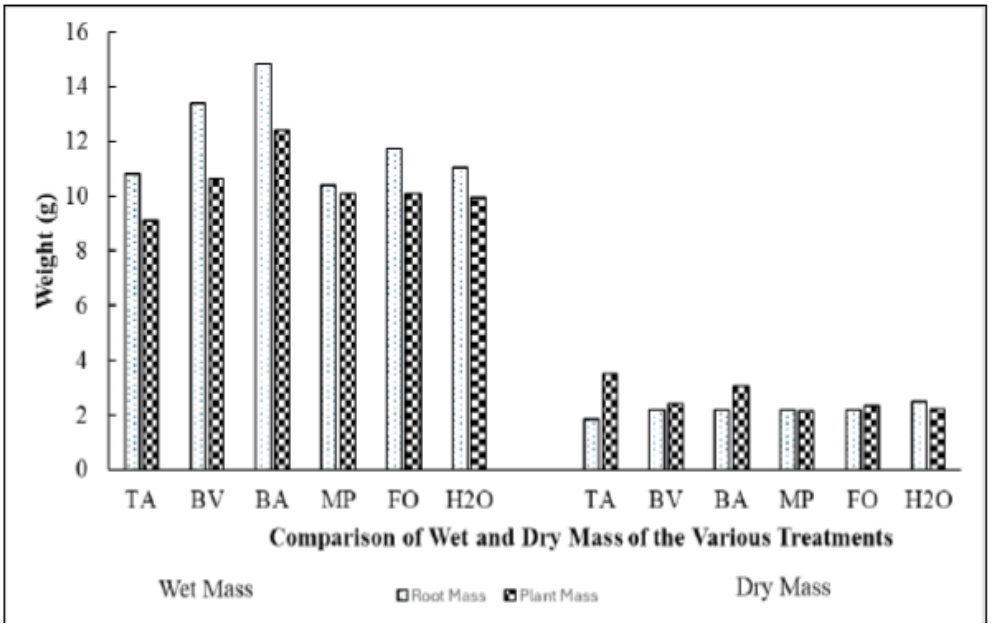

Figure 14 Comparison of Average Wet and Dry Plant Mass Across Various Treatments. The bar graph presents the average Wet Mass and Dry Mass (in grams, g) of the whole plant and roots for six different treatments (TA, BV, BA, MP, FO, and H2O). Within each treatment group, the solid bar represents Root Mass, and the patterned bar represents Plant Mass (shoot). The Wet Mass is significantly higher than the Dry Mass, consistent with water loss from drying the plant and root material for 48 hours in an oven at 65° C. The BA treatment generally resulted in the highest overall mass, both wet and dry, while the Dry Mass for the roots and plant across all treatments remained relatively consistent.

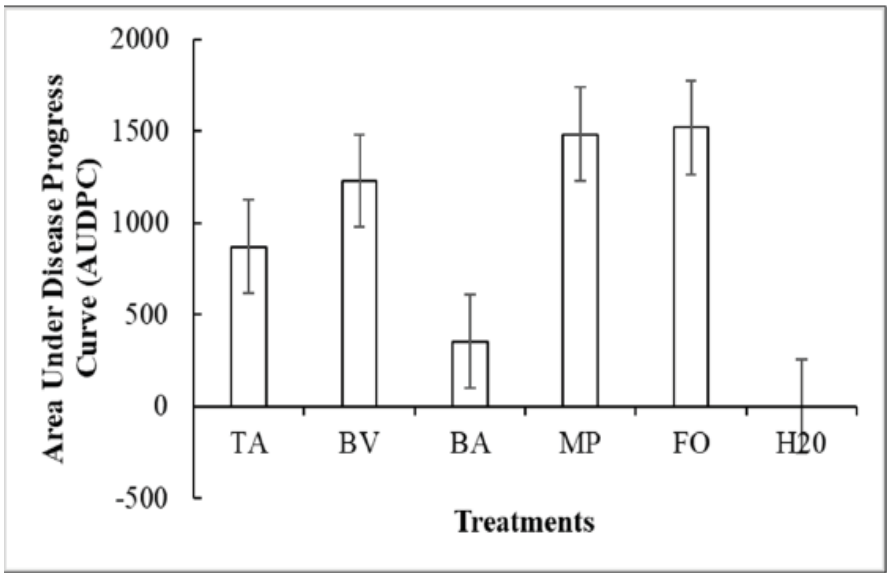

Figure 15 Area Under the Disease Progress Curve (AUDPC) for Various Treatments. The bar graph presents the AUDPC values for six different treatments (TA, BV, BA, MP, FO, and H2O). AUDPC is a measure of the cumulative disease severity over time, with lower values indicating greater disease control. The BA treatment exhibited the lowest positive AUDPC value, suggesting it provided the most effective disease control or suppression among the active treatments. Conversely, the FO and MP treatments resulted in the highest AUDPC values, indicating the greatest disease progression. The H2O control shows a value close to zero or slightly negative, which is unusual for an AUDPC calculation and may represent a baseline or a specific experimental result not following standard calculation conventions, or simply indicates minimal disease in the water control. The error bars represent the variability (e.g., standard deviation or standard error) associated with each mean AUDPC value.

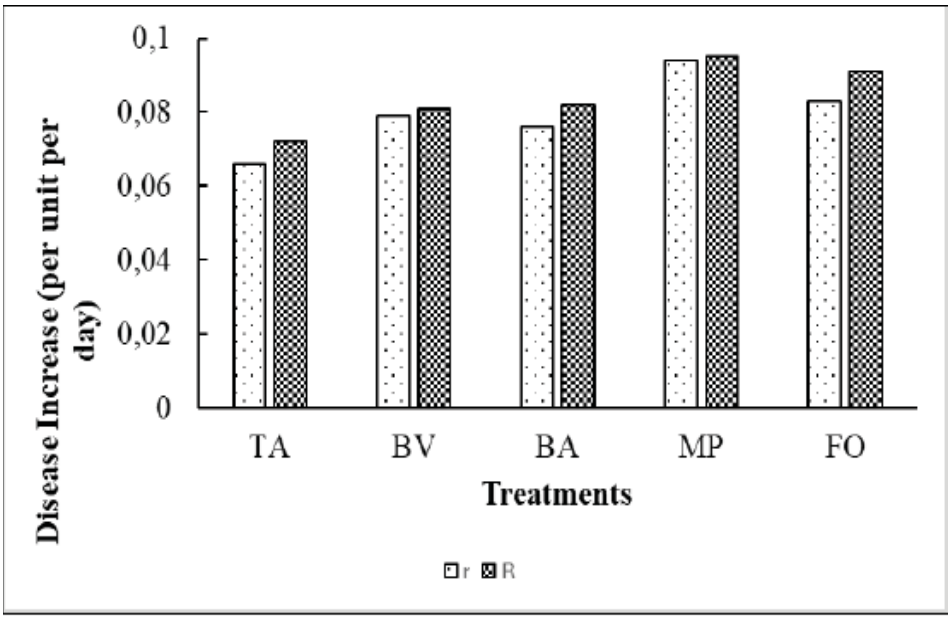

Figure 16 Comparison of Disease Increase Rates (r and R) for Various Treatments. The bar graph illustrates the rate of disease increase (expressed as per unit per) for five different treatments (TA, BV, BA, MP, and FO). The values for r (apparent infection rate, dotted bar) and R (maximum disease increase rate, patterned bar) are presented for each treatment. In all treatments, the R value is marginally higher than the corresponding r value. The MP treatment shows the highest rates for both r and R (approaching 0.1 per unit per day), indicating the fastest progression of the disease. The TA treatment shows the lowest rates for both r and R, suggesting it had the most significant effect in slowing the rate of disease spread compared to the other treatments.

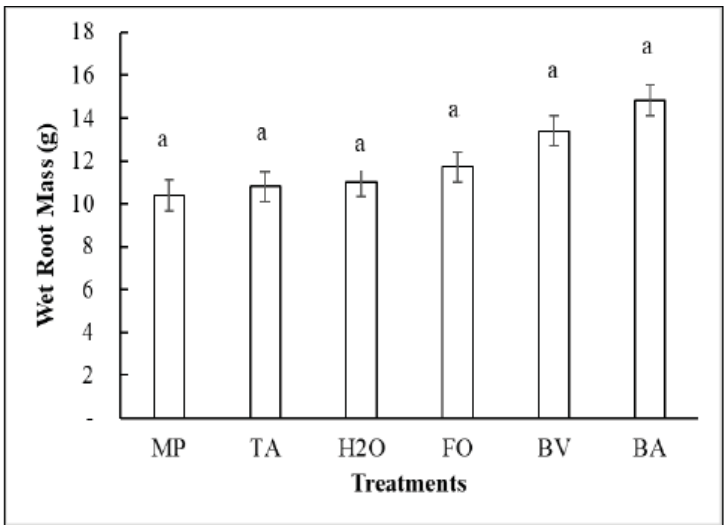

Figure 17 Mean root wet mass (g) of C. sativa under different treatments. Error bars represent the standard error of the mean (±SE). Bars with the same letter indicate no significant difference ($p > 0.05$) according to the Duncan's Multiple Range Test (DMRT).

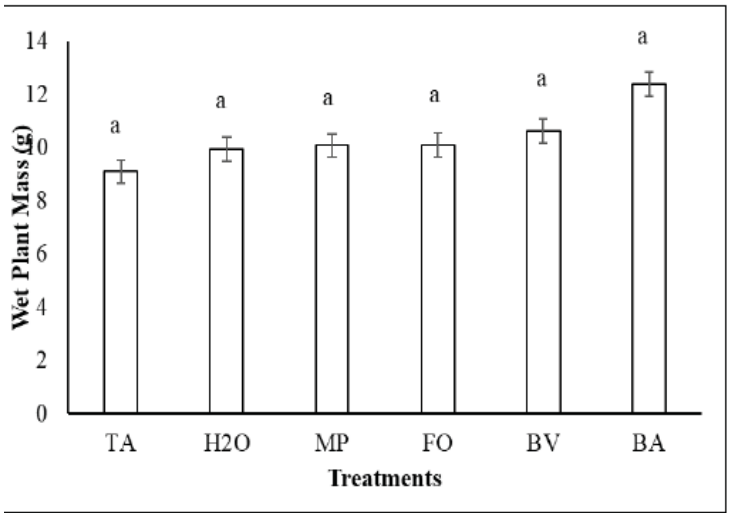

Figure 18 Mean plant wet mass (g) of C. sativa under different treatments. Error bars represent the standard error of the mean (±SE). Bars with the same letter indicate no significant difference ($p > 0.05$) according to the Duncan's Multiple Range Test (DMRT).

The present study shows that plant growth-promoting microorganisms can meaningfully suppress *Fusarium oxysporum* in *C. sativa*, but their effects are not uniform across *in vitro* and *in vivo* conditions. The dual-culture results in figure 1 and the bacterial antagonism setup in figure 2 showed that all four microorganisms inhibited pathogen growth, and the ANOVA confirmed highly significant treatment effects on mycelial growth at 3, 5 and 7 days. The SEM images strengthen this pattern: Figures 4 and 5 confirm the typical smooth, septate hyphae and

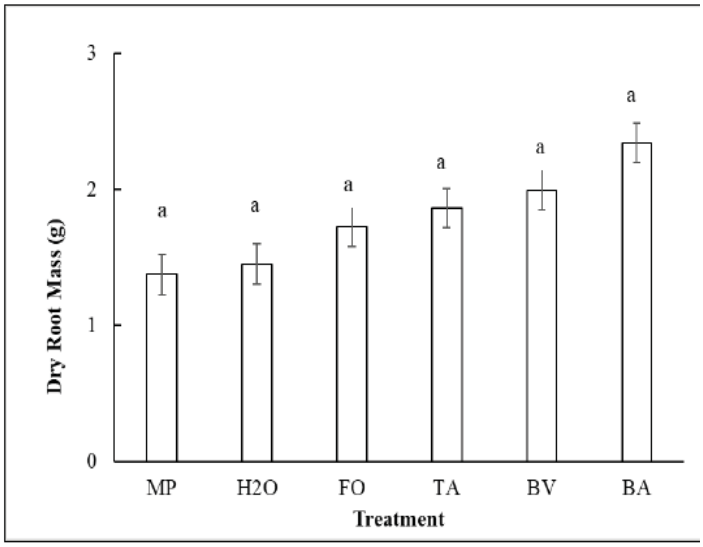

Figure 19 Mean root dry mass (g) of C. *sativa* under different treatments. Error bars represent the standard error of the mean (±SE). Bars with the same letter indicate no significant difference ($p > 0.05$) according to the Duncan's Multiple Range Test (DMRT).

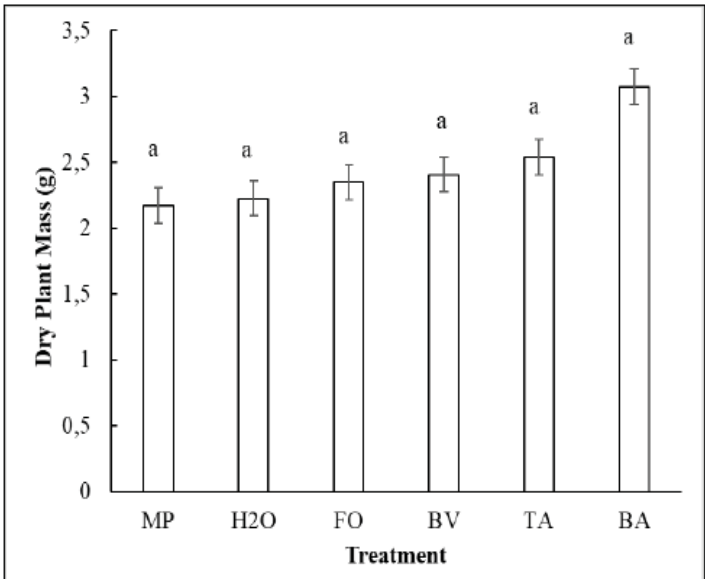

Figure 20 Shows the mean plant dry mass across treatments, with error bars representing the standard error of the mean. All treatments exhibited statistically similar dry mass values, as confirmed by DMRT ($p > 0.05$). The data indicate that treatment application had no substantial effect on dry biomass production in C. sativa. This suggests that, under the experimental conditions, the biological control agents neither enhanced nor reduced the accumulation of dry matter in the plants, and plant growth remained relatively uniform across treatments.

conidia of *F. oxysporum*, while figures 6 to 8 show hyphal coiling, surface colonisation, bacterial adhesion and biofilm-like material, all of which are consistent with direct antagonism rather than simple growth delay. This aligns well with previous microscopy work showing *Trichoderma asperellum* coiling around *Fusarium* hyphae and causing attachment and cell-wall disintegration [11,12], and with broader reviews describing biocontrol through direct antimicrobial activity,

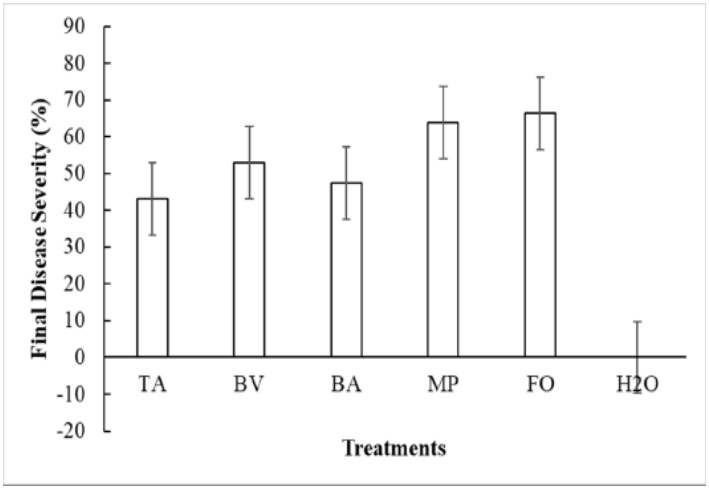

Figure 21 Effect of various treatments (e.g., T. *asperellum* (TA), B. *velezensis* (BV), B. *amyloliquefaciens* (BA), M. proteolyticum (MP), F. *oxysporum* (FO), and water control (H2O) on the final disease severity percentage of F. *oxyporum* in C. sativa. Error bars represent the standard error of the mean.

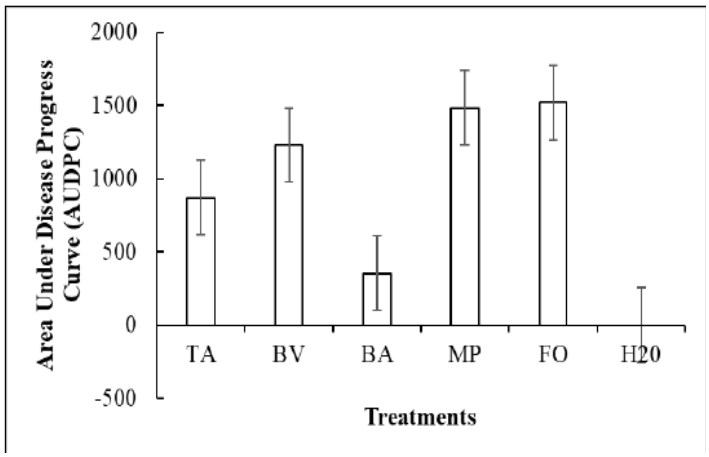

Figure 22 Area Under the Disease Progress Curve (AUDPC) values for C. *sativa* plants subjected to different treatments. Treatments include *Trichoderma asperellum* (TA), Bacillus velezensis (BV), *Bacillus amyloliquefaciens* (BA), *Microbacterium proteolyticum* (MP), *Fusarium oxysporum* inoculated positive control (FO), and water-treated negative control (H_2O). Error bars represent the standard deviation of the mean. Lower AUDPC values indicate reduced disease progression and improved disease suppression.

competition for space and nutrients, and induced resistance [5].

The SEM observations provide direct visual support for the antagonistic interactions between the tested microorganisms and *F. oxysporum*. In figures 4 and 5, the untreated fungal isolate displays the typical smooth, septate hyphae and conidia characteristic of *F. oxysporum*, providing a baseline morphology for comparison [13]. In contrast, figure 6 shows extensive hyphal coiling, intertwining, and surface colonization by *T. asperellum*, which is consistent with known Trichoderma mechanisms such as mycoparasitism, physical attachment to the pathogen, and close hyphal contact preceding lysis or structural disruption [12]. The abundance of *T. asperellum* conidia on and around the fungal hyphae further suggests active colonization and competition for space.

Figures 7 and 8 show a similarly intimate

Figure 23 Symptoms of Fusarium wilt on Bergville Cannabis species leaves in a greenhouse setting. Note the characteristic chlorosis (yellowing) and necrotic lesions (brown, dead spots) forming on the leaf margins and spreading inward.

association between *B. velezensis* and *F. oxysporum*, with bacterial cells densely adhering to the fungal surface and embedded in extracellular matrix material [14]. This biofilm-like structure is important because it may enhance persistence on the hyphal surface, improve colonization of the pathogen, and concentrate antimicrobial metabolites in the immediate vicinity of the fungus [14] The heavy coating of bacterial cells on fungal hyphae suggests that *B. velezensis* may suppress *F. oxysporum* through a combination of surface colonization, biofilm formation, nutrient competition, and secretion of antifungal compounds. Overall, the SEM images support the view that both *T. asperellum* and *B. velezensis* act through direct physical interaction with the pathogen, complementing the disease suppression observed in the greenhouse trials.

Among the fungal antagonists, *T. asperellum* behaved as expected for a classic mycoparasite: its inhibition was slower than that of the bacterial isolates, but the interaction zone and SEM images suggest that its mode of action depended on physical contact and hyphal parasitism rather than rapid overgrowth [15]. That interpretation is consistent with earlier cannabis and non-cannabis reports showing *Trichoderma* to be effective against *Fusarium* through pre-emptive colonisation and direct antagonism [4,6]. In greenhouse cannabis trials, *Trichoderma*-based products reduced *Fusarium* disease severity, although the effect depended on product and timing [1,4], which matches the observation that *T. asperellum* reduced disease progression but did not produce the strongest Area Under the Disease Progress Curve (AUDPC) reduction in this experiment.

The *Bacillus* treatments appear to be the strongest candidates overall for suppressing disease progression. In this greenhouse trial, *Bacillus amyloliquefaciens* gave the lowest AUDPC, while *B. velezensis* also reduced disease advancement and improved leaf number and vegetative vigour. That pattern is biologically plausible because *Bacillus* spp. are well known to act through lipopeptide production, antibiosis, competition and induced systemic resistance, and cannabis studies have already shown strong suppression of fungal pathogens by *Bacillus velezensis* and related strains [5,16,17]. In particular, cannabis-associated *Bacillus* isolates have previously shown clear inhibition of *F. oxysporum in vitro*, and *B. velezensis* has performed well against several cannabis fungal pathogens *in planta* [16], which supports the performance observed in figures 15 and 16.

The case of *Microbacterium proteolyticum* is more nuanced. It promoted the greatest plant height, yet it did not translate into the strongest disease suppression, suggesting that growth promotion and biocontrol were partly uncoupled under these experimental conditions. That is an important result, because it implies that a microbe can improve vegetative growth without necessarily providing the most reliable protection against *Fusarium* wilt. The biomass data in figures 17 to 20 support this interpretation: root wet mass, plant wet mass, root dry mass and total plant dry mass did not

differ significantly among treatments, so the clearest treatment effects were on disease development and some aboveground growth traits rather than final biomass accumulation. Under a 40-day greenhouse challenge, that is not surprising; disease suppression may need a longer period, lower inoculum pressure, or repeated application before it becomes visible as a biomass gain.

The disease progression graphs reinforce this picture. Figure 11 shows that disease severity increased in all inoculated groups, including those pretreated with antagonists, which means none of the biological agents fully prevented infection under the challenge conditions used here. What they did achieve was slowing the epidemic, and that is reflected most clearly in the lower AUDPC and slower disease increase rates for *B. amyloliquefaciens*, *T. asperellum* and *B. velezensis* in figures 15 and 16. In practical terms, this suggests that these agents are better interpreted as suppressive or protective inputs rather than as complete stand-alone controls. That conclusion fits the broader cannabis literature, where biopesticides are available but efficacy data are still limited, and where the best results have generally come from preventive rather than curative application [1,3,4].

Although the biological control agents reduced disease severity, some symptoms were still observed in treated plants because biocontrol suppression is rarely complete under high pathogen pressure, especially when inoculum loads are high or pathogen colonization has already been established before treatment. In addition, the effectiveness of biocontrol agents can be influenced by environmental conditions, colonization efficiency, and the timing of application relative to infection, which may allow residual symptom development despite treatment [4].

Taken together, the study adds useful crop-specific evidence for biological control in cannabis. The strongest overall message is that *B. amyloliquefaciens* and *B. velezensis* were the most effective suppressors of *F. oxysporum* disease progress in this system, while *T. asperellum* showed clear antagonistic capacity and *M. proteolyticum* appeared more growth-promoting than strongly protective. The figures make that pattern easy to follow: Figures 1, 2 and 6 to 8 document direct antagonism *in vitro*, figures 11, 15 and 16 show slowed disease development *in vivo*, and figures 17 to 20 show that these effects did not yet translate into significant differences in final biomass. That combination of findings suggests real promise, but also shows that strain identity, timing and formulation will matter if these microorganisms are to be used successfully in greenhouse cannabis production.

Conclusion

This study shows that plant growth-promoting microorganisms can suppress *Fusarium oxysporum* in *C. sativa*, although their effectiveness depends on the organism used. *Bacillus amyloliquefaciens* and *B. velezensis* gave the strongest disease suppression, while *Trichoderma asperellum* showed clear antagonistic activity and moderate control. *Microbacterium proteolyticum* improved plant height but did not provide comparable disease suppression, showing that growth promotion and biocontrol are not the same trait.

SEM and dual-culture results suggest that these antagonists act through different mechanisms, including adhesion, coiling, colonisation, and likely antibiosis. Although all inoculated plants eventually became diseased, the biological treatments slowed disease progress and reduced AUDPC relative to the pathogen control. Overall, these agents appear promising for integrated management of Fusarium wilt in cannabis, especially where chemical options are limited. However, the greenhouse setting, the limited set of antagonists tested, and the lack of long-term and field-scale data mean that further validation is needed before wider use.

Declarations

Funding

The authors declare that no funds, grants, or other support were received during the preparation of this manuscript.

Competing Interests

The authors have no relevant financial or non-financial interests to disclose.

Author Contributions

All authors contributed to the study conception and design. SM served as the main author, developed the methodology, and conducted the experimental work. NCM contributed as a co-author, providing critical proofreading and final edits. All authors have read and approved the final manuscript.

Ethics, Consent to Participate, and Consent to Publish declarations

Not applicable.

Data Availability

The datasets generated during and/or analysed during the current study are available from the corresponding author on reasonable request.

References

1. Punja ZK. Epidemiology of *Fusarium oxysporum* causing root and crown rot of cannabis (*Cannabis sativa* L., marijuana) plants in commercial greenhouse production. Can J Plant Pathol. 2021;43(2):216-235.
2. Buirs L, Punja ZK. Integrated management of pathogens and microbes in *Cannabis sativa* L. (Cannabis) under greenhouse conditions. Plants (Basel). 2024;13(6):786.
3. Gwinn KD, et al. Diseases of *Cannabis sativa* caused by diverse *Fusarium* species. Front Agron. 2022;3:796062.
4. Scott C, Punja ZK. Biological control of *Fusarium oxysporum* causing damping-off and *Pythium myriotylum* causing root and crown rot on cannabis (*Cannabis sativa* L.) plants. Can J Plant Pathol. 2023;45(3):238-252.
5. Boulahouat S, et al. Biocontrol efficiency of rhizospheric *Bacillus* against the plant pathogen *Fusarium oxysporum*: A promising approach for sustainable agriculture. Microbiol Res. 2023;14(3):892-908.
6. Pellegrini M, et al. *Fusarium oxysporum* f. sp. *cannabis* isolated from *Cannabis sativa* L.: In vitro and in planta biocontrol by a plant growth-promoting bacteria consortium. Plants (Basel). 2021;10(11):2436.
7. Franco-Correa M, Chavarro-Anzola V. Actinobacteria as plant growth-promoting. In: Dhanasekaran D, Jiang Y, editors. Actinobacteria: Basics and Biotechnological Applications. London: IntechOpen; 2016. p. 249.
8. Vaijayanthi G, Cholarajan A, Vijayakumar R. Isolation, characterization and antibacterial activity of terrestrial actinobacteria in the soils of Thanjavur district, Tamil Nadu, India. Res J Sci Technol. 2012;4(3):IV.
9. Antwi E. Antagonistic activity of secondary metabolites from rhizofunctional bacteria extracts against *Fusarium* species. Afr J Clin Exp Microbiol. 2024;25(1).
10. Kurmi S, et al. *Fusarium*: The versatile soil borne pathogen and its integrated management. J Adv Biol Biotechnol. 2025;28(11):143-158.
11. Elad Y, et al. Ultrastructural studies of the interaction between *Trichoderma* spp. and plant pathogenic fungi. J Phytopathol. 1983;107(2):168-175.
12. Sharma IP, Sharma AK. *Trichoderma-Fusarium* interactions: A biocontrol strategy to manage wilt. In: Sharma AK, Sharma IP, editors. Trichoderma: Host Pathogen Interactions and Applications. Singapore: Springer; 2020. p. 167-185.
13. Andargie YE, et al. Deciphering key factors in pathogen-suppressive microbiome assembly in the rhizosphere. Front Plant Sci. 2023;14:1301698.
14. Anusha B, et al. Evaluation of *Streptomyces* spp. and *Bacillus* spp. for biocontrol of *Fusarium* wilt in chickpea (*Cicer arietinum* L.). Arch Phytopathol Plant Prot. 2019;52(5-6):417-442.
15. Kumari R, et al. Synergistic effects of *Trichoderma* and biochar on the biocontrol of two soil-borne phytopathogens in chickpeas. Front Microbiol. 2025;16:1583114.
16. Kundy AC, et al. Building resilient crop production systems for drought-prone areas—a case for bambara groundnut (*Vigna subterranea* L. Verdc) and groundnut (*Arachis hypogaea* L.). Agronomy. 2023;13(2):383.
17. Gómez Expósito R, et al. Current insights into the role of rhizosphere bacteria in disease suppressive soils. Front Microbiol. 2017;8:2529.